

1 **TITLE PAGE**

2

3 **Type of article: Research article**

4

5 **Full-length title:**

6 **Culture and identification of a “Deltamicon” SARS-CoV-2 in a three cases cluster in**

7 **southern France**

8

9 **Short title (for the running head): Emergence of a SARS-CoV-2 Delta/Omicron**

10 **recombinant**

11

12 **Author list: Philippe COLSON<sup>1,2,3</sup>\*, Pierre-Edouard FOURNIER<sup>1,2,4</sup>, Jeremy**

13 **DELERCE<sup>1</sup>, Matthieu MILLION<sup>1,2,3</sup>, Marielle BEDOTTO<sup>1</sup>, Linda HOUHAMDI<sup>1</sup>,**

14 **Nouara YAHY<sup>5</sup>, Jeremy BAYETTE<sup>6</sup>, Anthony LEVASSEUR<sup>1,2</sup>, Jacques FANTINI<sup>5</sup>,**

15 **Didier RAOULT<sup>1,2</sup>, Bernard LA SCOLA<sup>1,2,3</sup>\***

16 **Affiliations:** <sup>1</sup> IHU Méditerranée Infection, 19-21 boulevard Jean Moulin, 13005 Marseille,

17 France; <sup>2</sup> Aix-Marseille Univ., Institut de Recherche pour le Développement (IRD), Microbes

18 Evolution Phylogeny and Infections (MEPHI), 27 boulevard Jean Moulin, 13005 Marseille,

19 France; <sup>3</sup> Assistance Publique-Hôpitaux de Marseille (AP-HM), 264 rue Saint-Pierre, 13005

20 Marseille, France; <sup>4</sup> Aix-Marseille Université, INSERM UMR S 1072, 51 boulevard Pierre

21 Dramard, 13015 Marseille, France; <sup>5</sup> Aix-Marseille Univ., Institut de Recherche pour le

22 Développement (IRD), Vecteurs – Infections Tropicales et Méditerranéennes (VITROME),

23 27 boulevard Jean Moulin, 13005 Marseille, France; <sup>6</sup> LBM Inovie Labosud, 90 rue Nicolas

24 Chedville, 34070, Montpellier, France.

25 **\* Corresponding author:** Bernard La Scola, IHU Méditerranée Infection, 19-21 boulevard

**NOTE: This preprint reports new research that has not been certified by peer review and should not be used to guide clinical practice.**

26 Jean Moulin, 13005 Marseille, France. Tel.: +33 413 732 401, Fax: +33 413 732 402; email:

27 [bernard.la-scola@univ-amu.fr](mailto:bernard.la-scola@univ-amu.fr); Philippe Colson, IHU Méditerranée Infection, 19-21

28 boulevard Jean Moulin, 13005 Marseille, France. Tel.: +33 413 732 401, Fax: +33 413 732

29 402; email: [philippe.colson@univ-amu.fr](mailto:philippe.colson@univ-amu.fr)

30 **Key words:** SARS-CoV-2; recombinant; variant; lineage; Delta; Omicron; Deltamicron;

31 epidemic

32 **Word counts:** abstract, 196; text, 2,560

33 **Figures:** 4; **Table:** 1; **References:** 43

34

35

36  
37  
38  
39  
40  
41  
42  
43  
44  
45  
46  
47  
48  
49  
50  
51  
52  
53  
54  
55

## ABSTRACT

Multiple SARS-CoV-2 variants have successively, or concomitantly spread worldwide since summer 2020. A few co-infections with different variants were reported and genetic recombinations, common among coronaviruses, were reported or suspected based on co-detection of signature mutations of different variants in a given genome. Here we report three infections in southern France with a Delta 21J/AY.4-Omicron 21K/BA.1 “Deltamicron” recombinant. The hybrid genome harbors signature mutations of the two lineages, supported by a mean sequencing depth of 1,163-1,421 reads and mean nucleotide diversity of 0.1-0.6%. It is composed of the near full-length spike gene (from codons 156-179) of an Omicron 21K/BA.1 variant in a Delta 21J/AY.4 lineage backbone. It is similar to those reported for 15 other patients sampled since January 2022 in Europe. Importantly, we cultured an isolate of this recombinant and sequenced its genome. It was observed by scanning electron microscopy. As it is misidentified with current variant screening qPCR, we designed and implemented for routine diagnosis a specific duplex qPCR. Finally, structural analysis of the recombinant spike suggested its hybrid content could optimize viral binding to the host cell membrane. These findings prompt further studies of the virological, epidemiological, and clinical features of this recombinant.

56

## TEXT

57

### 58 **Introduction**

59         The current SARS-CoV-2 pandemic has highlighted since the summer of 2020 the  
60 successive or concomittant emergence of numerous viral variants, each causing a specific  
61 epidemic (Lemey et al., 2021, Hodcroft et al., 2021; Colson et al., 2022b). Some of these  
62 variants spread to become pandemic while others remained epidemic in a restricted  
63 geographical area. The variants characterized so far have been shaped by nucleotide  
64 substitutions, insertions or deletions. However, another major evolutionary mechanism of  
65 RNA viruses is genetic recombination, which is very common among coronaviruses (Lai,  
66 1996; Zhang et al., 2015; Xiao et al., 2017; So et al., 2019; Gribble et al., 2021). It requires  
67 co-infection of the same host cell by two viruses, which may be two distinct mutants or  
68 variants (Bentley et al., 2018). Therefore, the frequency of creation of recombinants between  
69 two variants depends on the duration of their co-circulation, on the time until viral clearance,  
70 and on the number of people exposed to both viruses. Co-infections with two variants were  
71 reported including recently with SARS-CoV-2 Delta and Omicron variants (Jackson et al.,  
72 2021; Francisco et al., 2021; Taghizadeh et al., 2021; Rockett et al., 2022). Furthermore,  
73 genetic recombinations were reported or suspected, based on the concurrent detection in  
74 consensus genomes of signature mutations of different mutants or variants (Yi, 2020; Yeh and  
75 Contreras, 2020; VanInsberghe et al., 2020; Gallaher, 2020; Jackson et al., 2021; Haddad et  
76 al., 2021; Makarenkov et al., 2021; Varabyou et al., 2021; Leary et al., 2021; Taghizadeh et  
77 al., 2021; Lohrasbi-Nejad, 2022; Kreier, 2022; Ignatieva et al., 2022). A study detected up to  
78 1,175 (0.2%) putative recombinant genomes among 537,360 genomes from the GISAID  
79 database and estimated that up to 5% SARS-CoV-2 having circulated in the USA and UK  
80 could be recombinants (VanInsberghe et al., 2020).

81 Two pandemic variants, Delta and Omicron 21K [Nextclade classification  
82 (Aksamentov et al., 2021)]/BA.1 [Pangolin classification (Rambaut et al., 2020)], recently  
83 succeeded each other as the predominant viruses but co-circulated for a period of several  
84 weeks, creating conditions for co-infections and subsequently recombinations. This period  
85 spanned between December 27<sup>th</sup>, 2021 and February 14<sup>th</sup>, 2022 in our geographical area, as  
86 assessed by our SARS-CoV-2 genotypic surveillance based on variant-specific qPCR and  
87 next-generation genomic sequencing (Colson et al., 2022b; Colson et al., 2022a). In January  
88 2022, genomes harboring mutations from both Delta and Omicron 21K/BA.1 variants were  
89 reported in Cyprus but it was questioned whether sequences might have resulted from  
90 contamination (Kreier, 2022). Still, genomes being hybrids of these two variants and highly  
91 similar between each other were reported since February 2022, and their number in the  
92 GISAID database amounted to 15 as of 27/02/2022 ([https://github.com/cov-lineages/pango-](https://github.com/cov-lineages/pango-designation/issues/444)  
93 [designation/issues/444](https://github.com/cov-lineages/pango-designation/issues/444)). We herein report three infections by a recombinant SARS-CoV-2  
94 Delta 21K/AY.4-Omicron 21K/BA.1 whose genome is highly similar to the 15 previously  
95 reported genomes and the isolation of the recombinant virus from one of the patients.

96

## 97 **Materials and methods**

98 Nasopharyngeal samples were collected from two patients in our university hospital  
99 institute (Méditerranée Infection; <https://www.mediterranee-infection.com/>) and tested for  
100 SARS-CoV-2 infection by real-time reverse transcription-PCR (qPCR) as previously  
101 described (Colson et al., 2022b; Houhamdi et al., 2022). The third patient was sampled in a  
102 private medical biology laboratory in southern France (Inovie Labosud, Montpellier, France).  
103 qPCR assays that screen for SARS-CoV-2 variants were performed as recommended by  
104 French public health authorities ([https://www.data.gouv.fr/fr/datasets/donnees-de-](https://www.data.gouv.fr/fr/datasets/donnees-de-laboratoires-pour-le-depistage-indicateurs-sur-les-mutations/)  
105 [laboratoires-pour-le-depistage-indicateurs-sur-les-mutations/](https://www.data.gouv.fr/fr/datasets/donnees-de-laboratoires-pour-le-depistage-indicateurs-sur-les-mutations/)). In our center this included the

106 detection of spike mutation among which K417N (Thermo Fisher Scientific, Waltham, USA),  
107 combined with testing with the TaqPath COVID-19 kit (Thermo Fisher Scientific) that target  
108 viral genes ORF1, N (nucleocapsid) and S (spike), as previously reported (Colson et al.,  
109 2022b; Colson et al., 2022a). The private medical laboratory used the ID SARS-CoV-2/VOC  
110 Revolution Pentaplex assay (ID Solutions, Grabels, France) that detects spike mutations  
111 K417N, L452R, and E484K (Pentaplex assay, ID Solution, France).

112 SARS-CoV-2 genomes were sequenced in the framework of genomic surveillance  
113 implemented since February 2020 (Colson et al., 2022b) in our institute and as recommended  
114 by French public health authorities since 2021  
115 ([https://www.santepubliquefrance.fr/dossiers/coronavirus-covid-19/consortium-](https://www.santepubliquefrance.fr/dossiers/coronavirus-covid-19/consortium-emergen#block-356295)  
116 [emergen#block-356295](https://www.santepubliquefrance.fr/dossiers/coronavirus-covid-19/consortium-emergen#block-356295)). Next-generation sequencing was performed with the Illumina  
117 COVID-seq protocol on the NovaSeq 6000 instrument (Illumina Inc., San Diego, CA, USA)  
118 or with the Oxford Nanopore technology (ONT) on a GridION instrument (Oxford Nanopore  
119 Technologies Ltd., Oxford, UK) combined with prior multiplex PCR amplification according  
120 to the ARTIC procedure (<https://artic.network/>), as previously described (Colson et al.,  
121 2022b; Colson et al., 2022a), with the ARTIC nCoV-2019 Amplicon Panel v4.1 of primers  
122 (IDT, Coralville, IA, USA). Then, sequence read processing and genome analysis were  
123 performed as previously described (Colson et al., 2022b; Colson et al., 2022a). Briefly, for  
124 Illumina NovaSeq reads, base calling was performed with the Dragen Bcl Convert pipeline  
125 [v3.9.3; [https://emea.support.illumina.com/sequencing/sequencing\\_software/bcl-convert.html](https://emea.support.illumina.com/sequencing/sequencing_software/bcl-convert.html)  
126 (Illumina Inc.)], mapping was performed with the bwa-mem2 tool ([https://github.com/bwa-](https://github.com/bwa-mem2/bwa-mem2)  
127 [mem2/bwa-mem2](https://github.com/bwa-mem2/bwa-mem2)) on the Wuhan-Hu-1 isolate genome (GenBank accession no.  
128 NC\_045512.2) then cleaned with Samtools (<https://www.htslib.org/>), variant calling was  
129 carried out with freebayes (<https://github.com/freebayes/freebayes>) and consensus genomes  
130 were built using Bcftools (<https://samtools.github.io/bcftools/bcftools.html>). ONT reads were

131 processed with the ARTIC field bioinformatics pipeline (<https://github.com/artic->  
132 [network/fieldbioinformatics](https://github.com/artic-network/fieldbioinformatics)). Nucleotide and amino acid changes relatively to the Wuhan-  
133 Hu-1 isolate genome were obtained using the Nextclade tool (<https://clades.nextstrain.org/>)  
134 (Aksamentov et al., 2021; Rambaut et al., 2020). Nextstrain clades and Pangolin lineages  
135 were determined using the Nextclade web application (<https://clades.nextstrain.org/>)  
136 (Aksamentov et al., 2021) and the Pangolin tool (<https://cov-lineages.org/pangolin.html>)  
137 (Rambaut et al., 2020), respectively. Genome sequences described here were deposited in the  
138 GISAID sequence database (<https://www.gisaid.org/>) (EPI\_ISL\_10528736,  
139 EPI\_ISL\_10531214, EPI\_ISL\_10529499, EPI\_ISL\_10640045) (Alm et al., 2020). The  
140 Simplot software (<https://sray.med.som.jhmi.edu/SCSoftware/SimPlot/>) was used for  
141 recombination analysis. Phylogeny was reconstructed by the nextstrain/ncov tool  
142 (<https://github.com/nextstrain/ncov>) and visualized with Auspice  
143 (<https://docs.nextstrain.org/projects/auspice/en/stable/>). Genomes the closest genetically to  
144 those obtained here were selected among Delta 21J/AY.4 genomes recovered from GISAID  
145 based on their mutation pattern, then incorporated in the phylogeny together with the genome  
146 of the Wuhan-Hu-1 isolate.

147 SARS-CoV-2 culture isolation was performed by inoculating 200  $\mu$ L of respiratory  
148 sample on Vero E6 cells as previously described (La Scola et al., 2020). Cytopathic effect was  
149 observed by inverted microscopy. Viral particles were visualized in the culture supernatant by  
150 scanning electron microscopy with a SU5000 microscope (Hitachi High-Technologies  
151 Corporation, Tokyo, Japan), as previously described (Colson et al., 2020).

152 Structural predictions of the spike protein were performed as previously described  
153 (Fantini et al., 2021; Fantini et al., 2022; Colson et al., 2022a). Briefly, amino acid changes  
154 were introduced in the framework of a complete 14-1,200 structure of the original SARS-  
155 CoV-2 20B spike and missing amino acids were incorporated with the Robetta protein

156 structure prediction tool (<https://robetta.bakerlab.org/>) before energy minimization through  
157 the Polak-Ribière algorithm.

158 A in house duplex qPCR assay specific of the SARS-CoV-2 recombinant was  
159 designed that targets the genomes of the Delta 21J [targeted mutation: A11201G in the Nsp6  
160 gene (corresponding to amino acid substitution T77A)] and the Omicron 21K/BA.1 [targeted  
161 mutations: A23040G, G23048A, A23055G in the spike gene (Q493R, G496S, Q498R)]  
162 variants. The sequences of the primers and probes (in 5'-3' orientation) are as follows: (i) for  
163 the Delta 21J-targeting system: forward primer, CTGCTTTTGCAATGATGTTTGT; reverse  
164 primer, TACGCATCACCCAAGTAGCA; probe, 6FAM-  
165 CTTGCCGCTGTAGCTTATTTTAAT (primers and probe concentrations in the mix were  
166 200 nM and 150 nM, respectively); (ii) for the Omicron 21K/BA.1-targeting system: forward  
167 primer, CCTTGTAATGGTGTGAAGGTTTT; reverse primer,  
168 CTGGTGCATGTAGAAGTTCAAAAG; probe, 6VIC-  
169 TTTACGATCATATAGTTTCCGACCC (primers and probe concentrations in the mix were  
170 250 nM and 200 nM, respectively).

171 This study was approved by the ethics committee of University Hospital Institute  
172 Méditerranée Infection (No. 2022-001).

173

## 174 **Results**

175 The three case-patients were SARS-CoV-2-diagnosed on nasopharyngeal samples  
176 collected in February 2022. Cycle threshold values (Ct) of diagnostic qPCR were between 20-  
177 31. The patients were below 40 years of age. They resided in southern France and did not  
178 travel abroad recently. They presented mild respiratory symptoms. Two were vaccinated  
179 against SARS-CoV-2 (with two or three doses administered). Variant screening qPCR for the  
180 2 samples collected in our institute showed positivity for the K417N mutation while the



181 TaqPath COVID-19 kit (Thermo Fisher Scientific, Waltham, USA) provided positive signals  
182 for all three genes targeted (ORF1, S, and N). The third sample showed positivity for the  
183 K417N mutation and negativity for the L452R and E484K mutations. Thus, overall, qPCR  
184 carried out on the three samples were indicative of a Omicron variant.

185 Viral genomes (GISAID accession no. EPI\_ISL\_10528736, EPI\_ISL\_10531214, and  
186 EPI\_ISL\_10529499) from two of the three patients were identical and clustered in the  
187 phylogenetic analysis (**Figure 1**) despite no epidemiological link was documented between  
188 these two patients. The third genome exhibited 5 nucleotide differences. These 3 genomes  
189 were hybrids of Delta 21J AY.4 and Omicron 21K/BA.1 variant genomes (**Figure 2; Table**  
190 **1**). At positions harboring mutations compared to the genome of the Wuhan-Hu-1 isolate,  
191 mean sequencing depth was between 1,163-1,421 reads and mean prevalence of the  
192 majoritary nucleotide was between 99.4-99.9% (with minimum values between 80.3-98.7%),  
193 ruling out the concurrent presence of two variants in the samples either due to co-infection or  
194 to contamination. In addition, the 3 genomes were phylogenetically-related to 15 Delta  
195 21J/AY.4-Omicron 21K/BA.1 recombinant genomes previously detected in northern France,  
196 Denmark, and the Netherlands, and obtained from samples collected between January 3<sup>rd</sup>,  
197 2021 (in the French region Hauts-de-France) and February 16<sup>th</sup>, 2022 in Denmark (**Figure 1**).  
198 Phylogenetic analysis and time estimation based on estimated SARS-CoV-2 mutation rate [ $\approx$ 1  
199 mutation every 2 weeks (Van Dorp et al., 2020)] allowed estimating that the ancestor of this  
200 recombinant might have emerged in December 2021.

201 In this SARS-CoV-2 recombinant, most of the spike gene was replaced in a Delta  
202 21J/AY.4 matrix by an Omicron 21K/BA.1 sequence (**Figure 2**). Indeed, the recombination  
203 sites were located between nucleotide positions 22,029-22,034 and 22,097 for the first one,  
204 and between nucleotide positions 25,469 and 25,584 for the second one. These regions  
205 corresponds to amino acids 156 to 179 of the spike protein and to amino acids 26 to 64 of the

206 ORF3 protein whose gene is contiguous to the spike gene. The Simplot recombination  
207 analysis tool provided congruent results.

208 The respiratory sample from which the first recombinant genome was obtained was  
209 inoculated on Vero E6 cells the day following recombinant identification, and cytopathic  
210 effect was observed after 4 days (**Figures 3a, b**). The same day, supernatant was collected  
211 and next-generation genome sequencing was performed using Nanopore technology on a  
212 GridION instrument after PCR amplification with Artic primers, which allowed obtaining the  
213 genome sequence of the viral isolate 8 h later (GISAID accession no. EPI\_ISL\_10640045). At  
214 mutated positions compared to the Wuhan-Hu-1 isolate genome, mean sequencing depth was  
215 2,771 reads and mean prevalence of the majoritary nucleotide was 99.1% (minimum, 95.1%),  
216 and the consensus genome was identical to that obtained from the respiratory sample,  
217 showing unambiguously that the virus isolated was the Delta 21J/AY.4-Omicron 21K/BA.1  
218 recombinant. Finally, viral particles were observed in the culture supernatant by scanning  
219 electron microscopy with a SU5000 microscope within minutes after supernatant collection  
220 (**Figure 3c**).

221 The overall structure of the recombinant spike protein was predicted (**Figures 4a-c**).  
222 When superimposed with the spike of the Omicron 21K/BA.1 variant, the main structural  
223 changes were located in the N-terminal domain (NTD). In this region, the surface of the  
224 recombinant spike protein is enlarged, flattened, and more electropositive, a property that is  
225 characteristic of the Delta 21J/AY.4 NTD (**Figure 4c**). In the initial interaction of the virus  
226 with the plasma membrane of the host cells, the NTD is attracted by lipid rafts, which  
227 provides an electronegative landing platforms for the spike (Fantini et al., 2021; Fantini et al.,  
228 2022). Thus, an increase in the electrostatic surface of the NTD is expected to accelerate the  
229 binding of the virus to lipid rafts, which may confer a selective kinetic advantage against virus  
230 competitors (Fantini et al., 2021). The receptor binding domain (RBD) of the recombinant is

231 clearly inherited from the Omicron 21K/BA.1 variant (**Figure 4c**). The consequence is also an  
232 increase in the electrostatic surface potential of the RBD, which may facilitate the interaction  
233 with the electronegative interface of the ACE-2 cellular receptor. Overall, this structural  
234 analysis suggests that the recombinant virus could have been selected on the basis of kinetic  
235 properties conferred by a convergent increase of the electrostatic potential of both the NTD  
236 and the RBD, together with an enlargement of the NTD surface, all features that suggest an  
237 optimization of virus binding to the host cell membrane.

238         Currently used qPCR screening assays were not able to discriminate this Delta  
239 21J/AY.4-Omicron 21K/BA.1 recombinant and the Omicron 21K/BA.1 variant because the  
240 Delta variant signature mutation detected is absent from the recombinant genome. Therefore,  
241 we attempted to promptly implement a specific qPCR assay that could be used to detect the  
242 recombinant for routine diagnosis use. This was achieved in one day by selecting qPCR  
243 systems from our toolbox of dozens of in house qPCR systems that were designed since the  
244 emergence of the first variant during summer 2020 to specifically target SARS-CoV-2  
245 variants or mutants (Bedotto et al., 2021; Colson et al., 2022b). Two systems that target either  
246 the Delta 21J variant or the Omicron BA.1 variant were combined in a duplex qPCR that can  
247 screen for the recombinant. In preliminary assessment, both tested recombinant-positive  
248 samples were positive for the Delta 21J and Omicron BA.1 targets. In addition, 7 Delta non-  
249 21J-positive samples were negative for both targets, 4 Delta 21J-positive samples were  
250 positive for the Delta 21J target but negative for the Omicron BA.1 target, and 3 Omicron  
251 BA.1-positive samples were negative for the Delta 21J target but positive for the Omicron  
252 BA.1 target.

253

## 254 **Discussion**

255         It is increasingly demonstrated that the genomes of most biological entities, whatever

256 their level of complexity, are mosaics of sequences from various origins (Raoult, 2011;  
257 Merhej and Raoult, 2012; Feschotte et al., 2012; Roux et al., 2013; Jacobs et al., 2019). The  
258 present observations show us in real life the recombination potential of SARS-CoV-2, already  
259 largely established for other coronaviruses (Liu et al., 2013; Xiao et al., 2017; Lai, 1996;  
260 Zhang et al., 2015; Gribble et al., 2021) and reported or suspected for SARS-CoV-2 (Yi,  
261 2020; Yeh and Contreras, 2020; VanInsberghe et al., 2020; Gallaher, 2020; Jackson et al.,  
262 2021; Haddad et al., 2021; Varabyou et al., 2021; Leary et al., 2021; Taghizadeh et al., 2021;  
263 Lohrasbi-Nejad, 2022; Kreier, 2022; Ignatieva et al., 2022). SARS-CoV-2 recombinations  
264 were difficult to spot when only genetically very similar viruses were circulating, as was the  
265 case in Europe during the first epidemic episode with mutants derived from the Wuhan-Hu-1  
266 virus. The increasing genetic diversity of SARS-CoV-2, the tremendous number of infections  
267 at global and national levels, and the unprecedented global effort of genomic sequencing  
268 (<https://covariants.org/per-country>) (Aksamentov et al., 2022; Hodcroft et al., 2021; Alm et  
269 al., 2020; Colson et al., 2022b), raised the probability of detecting recombinants. Such  
270 observations will probably make it possible in the short or medium term to assess the  
271 recombination rate of SARS-CoV-2, whether there are recombination hotspots, and to what  
272 extent recombinations between different variants can generate new viable, and epidemic  
273 variants. This questions on the impact of recombinations on viral replication and  
274 transmissibility, and on clinical severity, as well as on the virus ability to escape neutralizing  
275 antibodies elicited by vaccines or a previous infection. In this view, culture isolation of  
276 SARS-CoV-2 recombinants as was carried out here for the first time to our knowledge is of  
277 primary importance. This will allow studying their phenotypic properties, among which their  
278 replicative capacity in various cell lines, their sensitivity to antibodies, or their genetic  
279 evolution *in vitro*. Concurrently, a high level of genomic surveillance must be maintained in  
280 order to detect and characterize all recombination events and circulating recombinants, which

281 is a critical scientific and public health issue.

282

283

## 284 **Acknowledgments**

285 We are very grateful to Clio Grimaldier, Rita Zgheib, Claudia Andrieu, Ludivine Bréchar, 286 and Raphael Tola for their technical help.

## 287 **Author contributions**

288 Study conception and design: Philippe Colson, Pierre-Edouard Fournier, Jacques Fantini, 289 Didier Raoult, Bernard La Scola. Materials, data and analysis tools: Philippe Colson, Pierre- 290 Edouard Fournier, Jeremy Delerce, Matthieu Million, Marielle Bedotto, Linda Houhamdi, 291 Nouara Yahi, Jeremy Bayette, Jacques Fantini. Data analyses: Philippe Colson, Pierre- 292 Edouard Fournier, Jeremy Delerce, Marielle Bedotto, Anthony Levasseur, Jacques Fantini, 293 Didier Raoult, Bernard La Scola. Writing of the first draft of the manuscript: Philippe Colson, 294 Jacques Fantini, and Pierre-Edouard Fournier. All authors read, commented on, and approved 295 the final manuscript.

## 296 **Funding**

297 This work was supported by the French Government under the “Investments for the Future” 298 program managed by the National Agency for Research (ANR), Méditerranée-Infection 10- 299 IAHU-03; by Région Provence Alpes Côte d’Azur and European funding FEDER PRIMMI 300 (Fonds Européen de Développement Régional-Plateformes de Recherche et d’Innovation 301 Mutualisées Méditerranée Infection), FEDER PA 0000320 PRIMMI; by Hitachi High- 302 Technologies Corporation, Tokyo, Japan; and by the French consortium on surveillance and 303 research on infections with emerging pathogens via microbial genomics (consortium relatif à 304 la surveillance et à la recherche sur les infections à pathogènes EMERgents via la

305 GENomique microbienne EMERGEN;  
306 <https://www.santepubliquefrance.fr/dossiers/coronavirus-covid-19/consortium-emergen>).

### 307 **Data availability**

308 The dataset generated and analyzed during the current study is available in the GISAID  
309 database (<https://www.gisaid.org/>).

### 310 **Conflicts of interest**

311 Didier Raoult has a conflict of interest as having been a consultant for Hitachi High-  
312 Technologies Corporation, Tokyo, Japan from 2018 to 2020. He is a scientific board member  
313 of Eurofins company and a founder of a microbial culture company (Culture Top). All other  
314 authors have no conflicts of interest to declare. Funding sources had no role in the design and  
315 conduct of the study; collection, management, analysis, and interpretation of the data; and  
316 preparation, review, or approval of the manuscript.

### 317 **Ethics**

318 This study has been approved by the ethics committee of the University Hospital Institute  
319 Méditerranée Infection (No. 2022-001). Access to the patients' biological and registry data  
320 issued from the hospital information system was approved by the data protection committee  
321 of Assistance Publique-Hôpitaux de Marseille (APHM) and was recorded in the European  
322 General Data Protection Regulation registry under number RGPD/APHM 2019-73.

323

324

325

326

## REFERENCES

- 327 Aksamentov I, Roemer C, Hodcroft EB, Neher RA. Nextclade: clade assignment, mutation  
328 calling and quality control for viral genomes. Zenodo 2021. doi:  
329 <https://doi.org/10.5281/zenodo.5607694>.
- 330 Alm E, Broberg EK, Connor T, Hodcroft EB, Komissarov AB, Maurer-Stroh S, Melidou A,  
331 Neher RA, O'Toole Á, Pereyaslov D; WHO European Region sequencing laboratories and  
332 GISAID EpiCoV group; WHO European Region sequencing laboratories and GISAID  
333 EpiCoV group. Geographical and temporal distribution of SARS-CoV-2 clades in the  
334 WHO European Region, January to June 2020. *Euro Surveill.* 2020 Aug;25(32):2001410.
- 335 Bedotto M, Fournier PE, Houhamdi L, Colson P, Raoult D. Implementation of an in-house  
336 real-time reverse transcription-PCR assay to detect the emerging SARS-CoV-2 N501Y  
337 variants. *J Clin Virol.* 2021;140:104868.
- 338 Bentley K, Evans DJ. Mechanisms and consequences of positive-strand RNA virus  
339 recombination. *J Gen Virol.* 2018;99:1345-1356.
- 340 Colson P, Delerce J, Beye M, Levasseur A, Boschi C, Houhamdi L, Tissot-Dupont H, Yahi  
341 N, Million M, La Scola B, Fantini J, Raoult D, Fournier PE. First cases of infection with  
342 the 21L/BA.2 Omicron variant in Marseille, France. medRxiv 2022a;  
343 2022.02.08.22270495; doi: <https://doi.org/10.1101/2022.02.08.22270495>.
- 344 Colson P, Fournier PE, Chaudet H, Delerce J, Giraud-Gatineau A, Houhamdi L, Andrieu C,  
345 Brechard L, Bedotto M, Prudent E, Gazin C, Beye M, Burel E, Dudouet P, Tissot-Dupont  
346 H, Gautret P, Lagier JC, Million M, Brouqui P, Parola P, Fenollar F, Drancourt M, La  
347 Scola B, Levasseur A, Raoult D. Analysis of SARS-CoV-2 variants from 24,181 patients  
348 exemplifies the role of globalization and zoonosis in pandemics. *Front Microbiol.*  
349 2022b;12:786233.
- 350 Colson P, Lagier JC, Baudoin JP, Bou Khalil J, La Scola B, Raoult D. Ultrarapid diagnosis,  
351 microscope imaging, genome sequencing, and culture isolation of SARS-CoV-2. *Eur J*  
352 *Clin Microbiol Infect Dis.* 2020 Aug;39(8):1601-1603.
- 353 Fantini J, Yahi N, Colson P, Chahinian H, La Scola B, Raoult D. The puzzling mutational  
354 landscape of the SARS-2-variant Omicron. *J Med Virol* 2022 Jan 8. doi:  
355 10.1002/jmv.27577. Epub ahead of print.
- 356 Fantini J, Yahi N, Azzaz F, Chahinian H. Structural dynamics of SARS-CoV-2 variants: A  
357 health monitoring strategy for anticipating Covid-19 outbreaks. *J Infect* 2021;83:197-206.
- 358 Feschotte C, Gilbert C. Endogenous viruses: insights into viral evolution and impact on host  
359 biology. *Nat Rev Genet.* 2012;13:283-96.
- 360 Francisco RDS Jr, Benites LF, Lamarca AP, de Almeida LGP, Hansen AW, Gularte JS,  
361 Demoliner M, Gerber AL, de C Guimarães AP, Antunes AKE, Heldt FH, Mallmann L,  
362 Hermann B, Ziulkoski AL, Goes V, Schallenberger K, Fillipi M, Pereira F, Weber MN, de  
363 Almeida PR, Fleck JD, Vasconcelos ATR, Spilki FR. Pervasive transmission of E484K  
364 and emergence of VUI-NP13L with evidence of SARS-CoV-2 co-infection events by two  
365 different lineages in Rio Grande do Sul, Brazil. *Virus Res.* 2021;296:198345.

- 366 Gallaher WR. A palindromic RNA sequence as a common breakpoint contributor to copy-  
367 choice recombination in SARS-COV-2. *Arch Virol.* 2020;165:2341-2348.
- 368 Gribble J, Stevens LJ, Agostini ML, Anderson-Daniels J, Chappell JD, Lu X, Pruijssers AJ,  
369 Routh AL, Denison MR. The coronavirus proofreading exoribonuclease mediates  
370 extensive viral recombination. *PLoS Pathog.* 2021;17(1):e1009226.
- 371 Haddad D, John SE, Mohammad A, Hammad MM, Hebbar P, Channanath A, Nizam R, Al-  
372 Qabandi S, Al Madhoun A, Alshukry A, Ali H, Thanaraj TA, Al-Mulla F. SARS-CoV-2:  
373 Possible recombination and emergence of potentially more virulent strains. *PLoS One.*  
374 2021;16:e0251368.
- 375 Hadfield J, Megill C, Bell SM, Huddleston J, Potter B, Callender C, Sagulenko P, Bedford T,  
376 Neher RA. Nextstrain: real-time tracking of pathogen evolution. *Bioinformatics.*  
377 2018;34:4121-4123.
- 378 Hodcroft EB, Zuber M, Nadeau S, Vaughan TG, Crawford KHD, Althaus CL, Reichmuth  
379 ML, Bowen JE, Walls AC, Corti D, Bloom JD, Velesler D, Mateo D, Hernando A, Comas  
380 I, González Candelas F; SeqCOVID-SPAIN consortium, Stadler T, Neher RA. Emergence  
381 and spread of a SARS-CoV-2 variant through Europe in the summer of 2020. *Nature.*  
382 2021;595:707-712.
- 383 Houhamdi L, Gautret P, Hoang VT, Fournier PE, Colson P, Raoult D. Characteristics of the  
384 first 1119 SARS-CoV-2 Omicron variant cases, in Marseille, France, November-December  
385 2021. *J Med Virol.* 2022 Jan 20. doi: 10.1002/jmv.27613. Epub ahead of print.
- 386 Hodcroft E. 2012. CoVariants: SARS-CoV-2 mutations and variants of interest. Available  
387 from: <https://covariants.org/>.
- 388 Ignatieva A, Hein J, Jenkins PA. Ongoing recombination in SARS-CoV-2 revealed through  
389 genealogical reconstruction. *Mol Biol Evol.* 2022;39:msac028.
- 390 Jackson B, Boni MF, Bull MJ, Colleran A, Colquhoun RM, Darby AC, Haldenby S, Hill V,  
391 Lucaci A, McCrone JT, Nicholls SM, O'Toole Á, Pacchiarini N, Poplawski R, Scher E,  
392 Todd F, Webster HJ, Whitehead M, Wierzbicki C; COVID-19 Genomics UK (COG-UK)  
393 Consortium, Loman NJ, Connor TR, Robertson DL, Pybus OG, Rambaut A. Generation  
394 and transmission of interlineage recombinants in the SARS-CoV-2 pandemic. *Cell.*  
395 2021;184:5179-5188.e8.
- 396 Jacobs GS, Hudjashov G, Saag L, Kusuma P, Darusallam CC, Lawson DJ, Mondal M, Pagani  
397 L, Ricaut FX, Stoneking M, Metspalu M, Sudoyo H, Lansing JS, Cox MP. Multiple deeply  
398 divergent Denisovan ancestries in Papuans. *Cell.* 2019;177:1010-1021.e32.
- 399 Kreier F. Deltacron: the story of the variant that wasn't. *Nature.* 2022;602:19.
- 400 La Scola B, Le Bideau M, Andreani J, Hoang VT, Grimaldier C, Colson P, Gautret P, Raoult  
401 D. Viral RNA load as determined by cell culture as a management tool for discharge of  
402 SARS-CoV-2 patients from infectious disease wards. *Eur J Clin Microbiol Infect Dis.*  
403 2020;39:1059-1061.



- 404 Lai MMC. Recombination in large RNA viruses: Coronaviruses. *Semin Virol.* 1996;7:381-  
405 388.
- 406 Leary S, Gaudieri S, Parker MD, Chopra A, James I, Pakala S, Alves E, John M, Lindsey BB,  
407 Keeley AJ, Rowland-Jones SL, Swanson MS, Ostrov DA, Bubenik JL, Das S, Sidney J,  
408 Sette A; COVID-19 Genomics UK (COG-UK) consortium, de Silva TI, Phillips E, Mallal  
409 S. Generation of a novel SARS-CoV-2 sub-genomic RNA due to the R203K/G204R  
410 variant in nucleocapsid: homologous recombination has potential to change SARS-CoV-2  
411 at both protein and RNA level. *Pathog Immun.* 2021;6:27-49.
- 412 Lemey P, Ruktanonchai N, Hong SL, Colizza V, Poletto C, Van den Broeck F, Gill MS, Ji X,  
413 Levasseur A, Oude Munnink BB, Koopmans M, Sadilek A, Lai S, Tatem AJ, Baele G,  
414 Suchard MA, Dellicour S. Untangling introductions and persistence in COVID-19  
415 resurgence in Europe. *Nature.* 2021;595:713-717.
- 416 Liu X, Shao Y, Ma H, Sun C, Zhang X, Li C, Han Z, Yan B, Kong X, Liu S. Comparative  
417 analysis of four Massachusetts type infectious bronchitis coronavirus genomes reveals a  
418 novel Massachusetts type strain and evidence of natural recombination in the genome.  
419 *Infect Genet Evol.* 2013;14:29-38.
- 420 Lohrasbi-Nejad A. Detection of homologous recombination events in SARS-CoV-2.  
421 *Biotechnol Lett.* 2022 Jan 17:1–16. doi: 10.1007/s10529-021-03218-7. Epub ahead of  
422 print.
- 423 Makarenkov V, Mazouze B, Rabusseau G, Legendre P. Horizontal gene transfer and  
424 recombination analysis of SARS-CoV-2 genes helps discover its close relatives and shed  
425 light on its origin. *BMC Ecol Evol.* 2021;21:5.
- 426 Merhej V, Raoult D. Rhizome of life, catastrophes, sequence exchanges, gene creations, and  
427 giant viruses: how microbial genomics challenges Darwin. *Front Cell Infect Microbiol.*  
428 2012;2:113.
- 429 Rambaut A, Holmes EC, O'Toole Á, Hill V, McCrone JT, Ruis C, du Plessis L, Pybus OG. A  
430 dynamic nomenclature proposal for SARS-CoV-2 lineages to assist genomic  
431 epidemiology. *Nat Microbiol.* 2020;5:1403-1407.
- 432 Raoult D. A viral grandfather: genomics in 2010 contradict Darwin's vision of evolution. *Eur*  
433 *J Clin Microbiol Infect Dis.* 2011;30:935-6.
- 434 Rockett, Jenny Draper, Mailie Gall, Eby M Sim, Alicia Arnott, Jessica E Agius, Jessica  
435 Johnson-Mackinnon, Elena Martinez, Alexander P Drew, Clement Lee, Christine Ngo,  
436 Marc Ramsperger, Andrew N Ginn, Qinning Wang, Michael Fennell, Danny Ko, Linda  
437 Huston, Lukas Kairaitis, Edward C Holmes, Matthew N O'Sullivan, Sharon C-A Chen, Jen  
438 Kok, Dominic E Dwyer, Vitali Sintchenko. Co-infection with SARS-CoV-2 Omicron and  
439 Delta Variants revealed by genomic surveillance. *medRxiv* 2022; 2022.02.13.22270755;  
440 doi: <https://doi.org/10.1101/2022.02.13.22270755>.
- 441 Roux S, Enault F, Bronner G, Vaultot D, Forterre P, Krupovic M. Chimeric viruses blur the  
442 borders between the major groups of eukaryotic single-stranded DNA viruses. *Nat*  
443 *Commun.* 2013;4:2700.

- 444 So RTY, Chu DKW, Miguel E, Perera RAPM, Oladipo JO, Fassi-Fihri O, Aylet G, Ko RLW,  
445 Zhou Z, Cheng MS, Kuranga SA, Roger FL, Chevalier V, Webby RJ, Woo PCY, Poon  
446 LLM, Peiris M. Diversity of dromedary camel coronavirus HKU23 in African camels  
447 revealed multiple recombination events among closely related betacoronaviruses of the  
448 subgenus Embecovirus. *J Virol.* 2019;93:e01236-19.
- 449 Taghizadeh P, Salehi S, Heshmati A, Houshmand SM, InanlooRahatloo K, Mahjoubi F,  
450 Sanati MH, Yari H, Alavi A, Jamehdar SA, Dabiri S, Galehdari H, Haghshenas MR,  
451 Hashemian AM, Heidarzadeh A, Jahanzad I, Kheyraani E, Piroozmand A, Mojtahedi A,  
452 Nikoo HR, Rahimi Bidgoli MM, Rezvani N, Sepehrnejad M, Shakibzadeh A, Shariati G,  
453 Seyyedi N, MohammadSaleh Zahraei S, Safari I, Elahi E. Study on SARS-CoV-2 strains in  
454 Iran reveals potential contribution of co-infection with and recombination between  
455 different strains to the emergence of new strains. *Virology.* 2021;562:63-73.
- 456 van Dorp L, Richard D, Tan CCS, Shaw LP, Acman M, Balloux F. No evidence for increased  
457 transmissibility from recurrent mutations in SARS-CoV-2. *Nat Commun.* 2020;11:5986.
- 458 VanInsberghe D, Neish AS, Lowen AC, Koelle K. Recombinant SARS-CoV-2 genomes are  
459 currently circulating at low levels. *bioRxiv* 2021;2020.08.05.238386. doi:  
460 10.1101/2020.08.05.238386.
- 461 Varabyou A, Pockrandt C, Salzberg SL, Pertea M. Rapid detection of inter-clade  
462 recombination in SARS-CoV-2 with Bolotie. *Genetics.* 2021;218:iyab074.
- 463 Xiao Y, Rouzine IM, Bianco S, Acevedo A, Goldstein EF, Farkov M, Brodsky L, Andino R.  
464 RNA recombination enhances adaptability and is required for virus spread and virulence.  
465 *Cell Host Microbe.* 2017;22:420.
- 466 Yeh TY, Contreras GP. Emerging viral mutants in Australia suggest RNA recombination  
467 event in the SARS-CoV-2 genome. *Med J Aust.* 2020;213:44-44.e1.
- 468 Yi H. 2019 Novel coronavirus is undergoing active recombination. *Clin Infect Dis.*  
469 2020;71:884-887.
- 470 Zhang Y, Li J, Xiao Y, Zhang J, Wang Y, Chen L, Paranhos-Baccalà G, Ren L, Wang J.  
471 Genotype shift in human coronavirus OC43 and emergence of a novel genotype by natural  
472 recombination. *J Infect.* 2015;70:641-50.

473

474

475

476

## FIGURE LEGEND

477

478 **Figure 1. Phylogeny reconstruction based on SARS-CoV-2 Delta 21J/AY.4-Omicron**

479 **21K/BA.1 genomes.**

480 Phylogenetic analysis was performed using the nextstrain/ncov tool

481 (<https://github.com/nextstrain/ncov>) then visualized with Auspice

482 (<https://docs.nextstrain.org/projects/auspice/en/stable/>). X-axis shows time. Sequences are

483 labelled with GISAID identifiers (<https://www.gisaid.org/>) (Alm et al., 2020).

484

485 **Figure 2. Schematic of the SARS-CoV-2 Delta 21J/AY.4-Omicron 21K/BA.1**

486 **recombinant genome.**

487 a. Map of the SARS-CoV-2 genome.

488 b. Schematic representation of parental and recombinant genomes.

489 c. Mutations in the three Delta 21J/AY.4-Omicron 21K/BA.1 recombinant genomes. Adapted

490 from screenshots of the nextclade web application output (<https://clades.nextstrain.org>)

491 (Hadfield et al., 2018; Aksamentov et al., 2021). Color codes for nucleotide mutations and are

492 marked regions as follows: Green: U; yellow: G; blue: C; red: A; grey: deletions or uncovered

493 regions.

494

495 **Figure 3. Microscopy images of the virus cytopathic effect (a, b) and of a viral particle**

496 **(c) in culture of the SARS-CoV-2 Delta 21J/AY.4-Omicron 21K/BA.1 recombinant on**

497 **Vero E6 cells.**

498 a. Absence of cytopathic effect (negative control: absence of virus); b. Cytopathic effect

499 observed 4 days post-inoculation on Vero E6 cells of the respiratory sample of the first patient

500 for whom the SARS-CoV-2 Delta 21J/AY.4-Omicron 21K/BA.1 recombinant was identified.

501 c. Scanning electron microscopy image was obtained with a SU5000 microscope (Hitachi  
502 High-Technologies Corporation, Tokyo, Japan).

503

504 **Figure 4. Schematic of the predicted structure of the spike protein of the SARS-CoV-2**  
505 **Delta 21J/AY.4-Omicron 21K/BA.1 recombinant**

506 a. Overall structure of the recombinant spike protein. The secondary structure is in grey,  
507 mutated amino acids are in blue. NTD, N-terminal domain; RBD, receptor binding domain;  
508 S1-S2, cleavage site.

509 b. Superimposition of the secondary structure of the Omicron 21K/BA.1 variant (in cyan) and  
510 recombinant (in red) spike proteins. NTD, N-terminal domain; RBD, receptor binding  
511 domain.

512 c. Comparison of the electrostatic surface potential of the spike proteins in Delta 21J/AY.4  
513 lineage, Omicron 21K/BA.1 variant, and in the recombinant. The color scale (negative in red,  
514 positive in blue, neutral in white) is indicated. NTD, N-terminal domain; RBD, receptor  
515 binding domain.

516

517

518

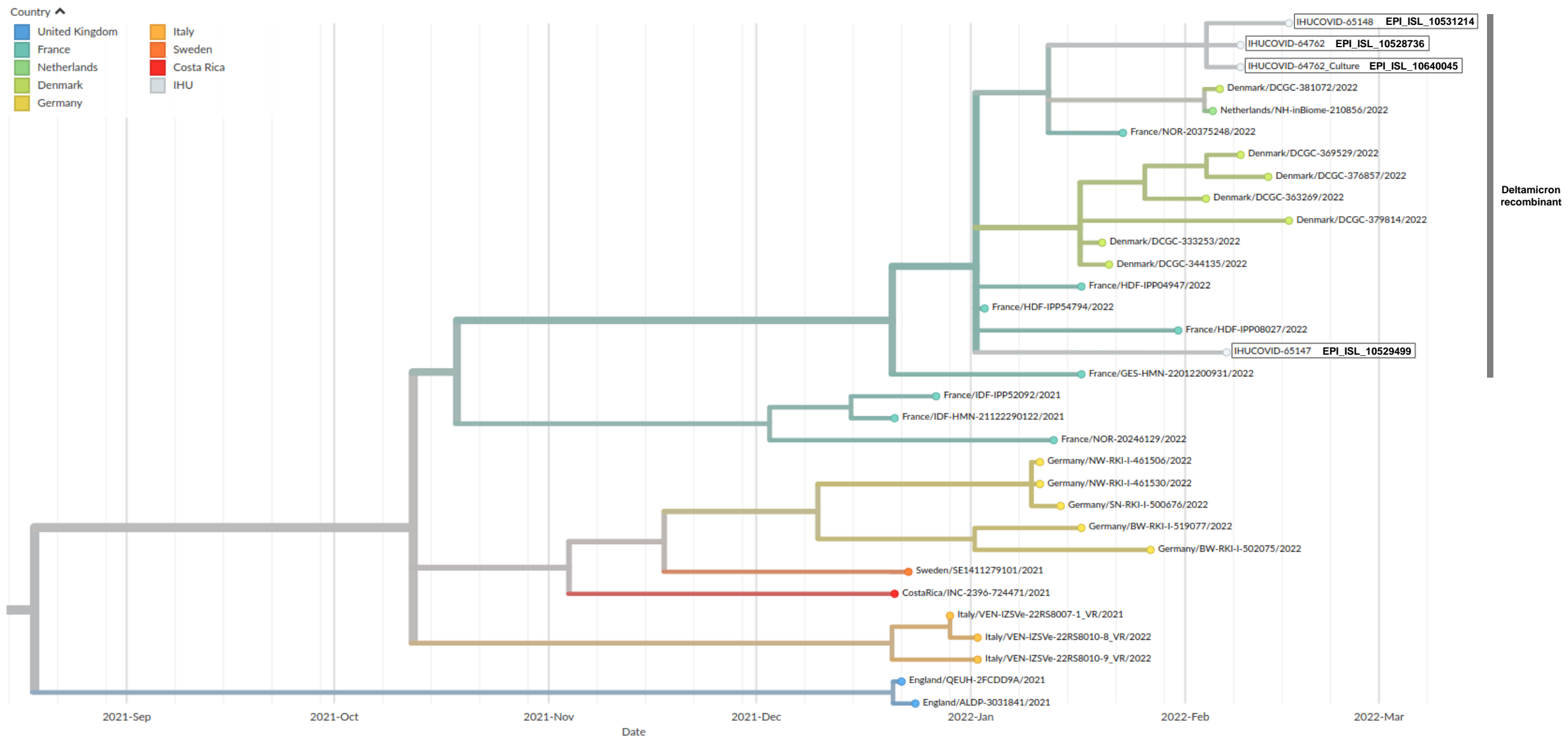
**TABLE**

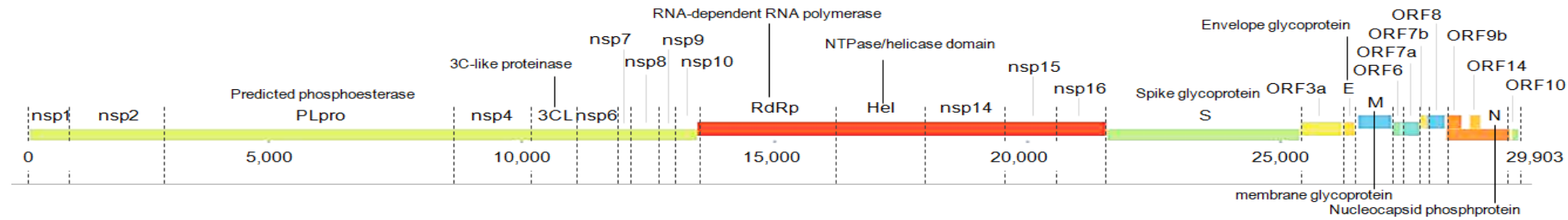
519 **Table 1. Nucleotide and amino acid changes in the Deltamicron recombinant according to**  
 520 **their presence/absence in the Delta 21J/AY.4 lineage and the Omicron 21K/BA.1**  
 521

SARS-CoV-2 genes or genome regions	Nucleotide changes	Amino acid changes	Specific of the Delta 21J/AY.4 lineage ancestor before recombination	Present in the Delta 21J/AY.4 lineage	Present in the Omicron 21K/BA.1 variant
5'UTR	G210U	/		X	
5'UTR	C241U	/		X	X
ORF1a	A1321C	E352D	X		
ORF1a	C3037U	/		X	X
ORF1a	G4181U	A1306S		X	
ORF1a	C6402U	P2046L		X	
ORF1a	C7124U	P2287S		X	
ORF1a	C7851U	A2529V		X	
ORF1a	A8723G	I2820V	X		
ORF1a	C8986U	/		X	
ORF1a	G9053U	V2930L		X	
ORF1a	C10029U	T3255I		X	X
ORF1a	A11201G	T3646A		X	
ORF1a	A11332G	/		X	
ORF1b	C14407U	P314F		X	X
ORF1b	C14408U	P314F		X	X
ORF1b	U15264C	/	X		
ORF1b	G15451A	G662S		X	
ORF1b	C16466U	P1000L		X	
ORF1b	C19220U	A1918V		X	
S	C21618G	T19R		X	
S	G21641U	A27S	X		
S	C21846U	T95I		X	X
S	G21987A	G142D		X	
S	GAGUUCA22028G	EFR156G		X	
S	AAUU22193A	NL211I			X
S	U22204UGAGCCAGAA	INS214EPE			X
S	G22578A	G339D			X
S	UC22673CU	S371L			X
S	U22679C	S373P			X
S	C22686U	S375F			X
S	G22813U	K417N			X
S	U22882G	N440K			X
S	G22898A	G446S			X
S	G22992A	S477N			X
S	C22995A	T478K		X	X
S	A23013C	E484A			X
S	A23040G	Q493R			X
S	G23048A	G496S			X
S	A23055G	Q498R			X
S	A23063U	N501Y			X
S	U23075C	Y505H			X
S	C23202A	T547K			X
S	A23403G	D614G		X	X
S	C23525U	H655Y			
S	U23599G	N679K			X
S	C23604A	P681H			X
S	C23854A	N764K			X
S	G23948U	D796Y			X
S	C24130A	N856K			X
S	A24424U	O954H			X
S	U24469A	N969K			X
S	C24503U	L981F			X
S	C25000U	/			X
ORF3a	C25667U	S92L	X		
ORF3a	G25855U	D155Y	X		
M	U26767C	I82T		X	
ORF7a	U27638C	V82A		X	
ORF7a	C27752U	T120I		X	
ORF7b	C27874U	T40I		X	
ORF8	AGAUUUC28247A	DF119Del		X	
Intergenic region	UA28270U	/		X	
N	A28461G	D63G		X	
N	G28881U	R203M		X	
N	G28916U	G215C		X	
N	G29402U	D377Y		X	
Intergenic region	G29540A	/	X		
ORF10	G29645U	/	X		
3'UTR	G29742U	/		X	

522 /, no change; X, present; UTR, untranslated region; S gene region is indicated by a grey background

Fig. 1



**Fig. 2****a. Map of the SARS-CoV-2 genome****b. Schematic of parental and recombinant genomes**

Parental Delta 21J AY.4 genome



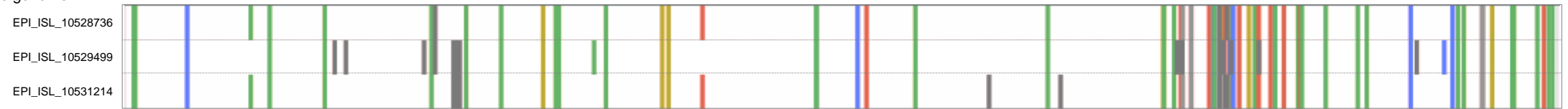
Delta 21J AY.4 - Omicron 21K/BA1 recombinant genomes



Parental Omicron 21K/BA.1 genome

**c. Nucleotide mutations in the three Delta 21J AY.4 / Omicron 21K/BA1 recombinant genomes**

relatively to Wuhan-Hu-1 isolate genome



relatively to Delta 21J AY.4 variant genome



relatively to Omicron 21K/BA.1 variant genome

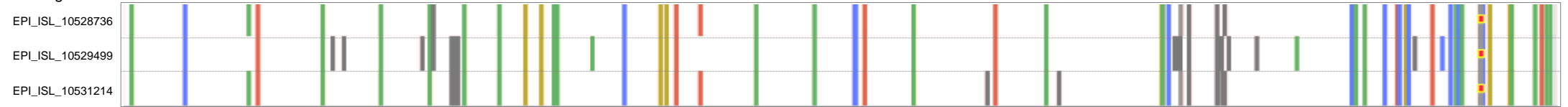
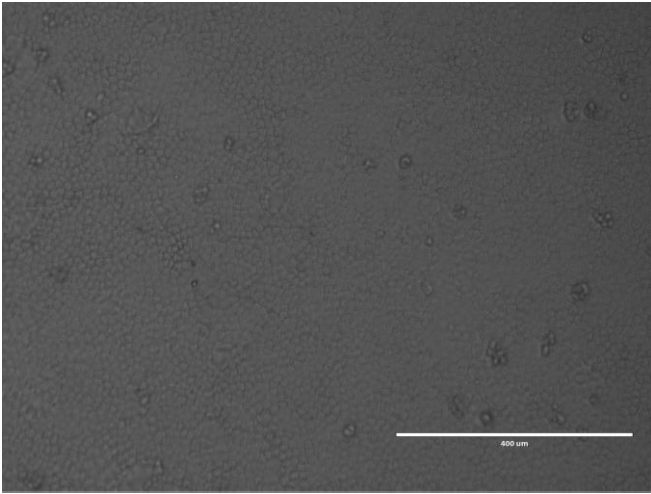
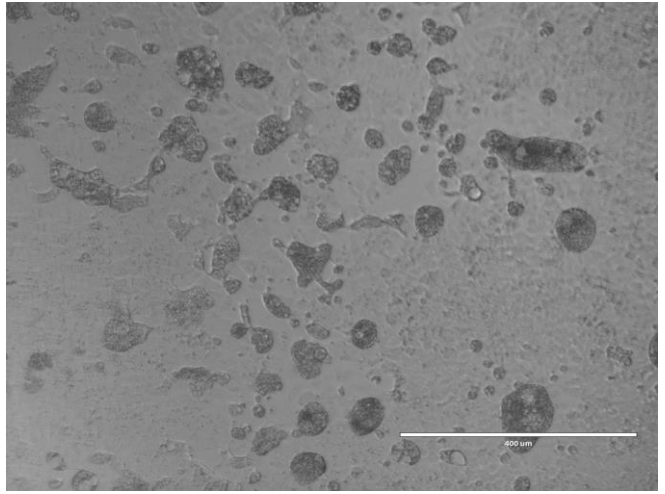


**Fig. 3**

**a.**



**b.**



**c.**

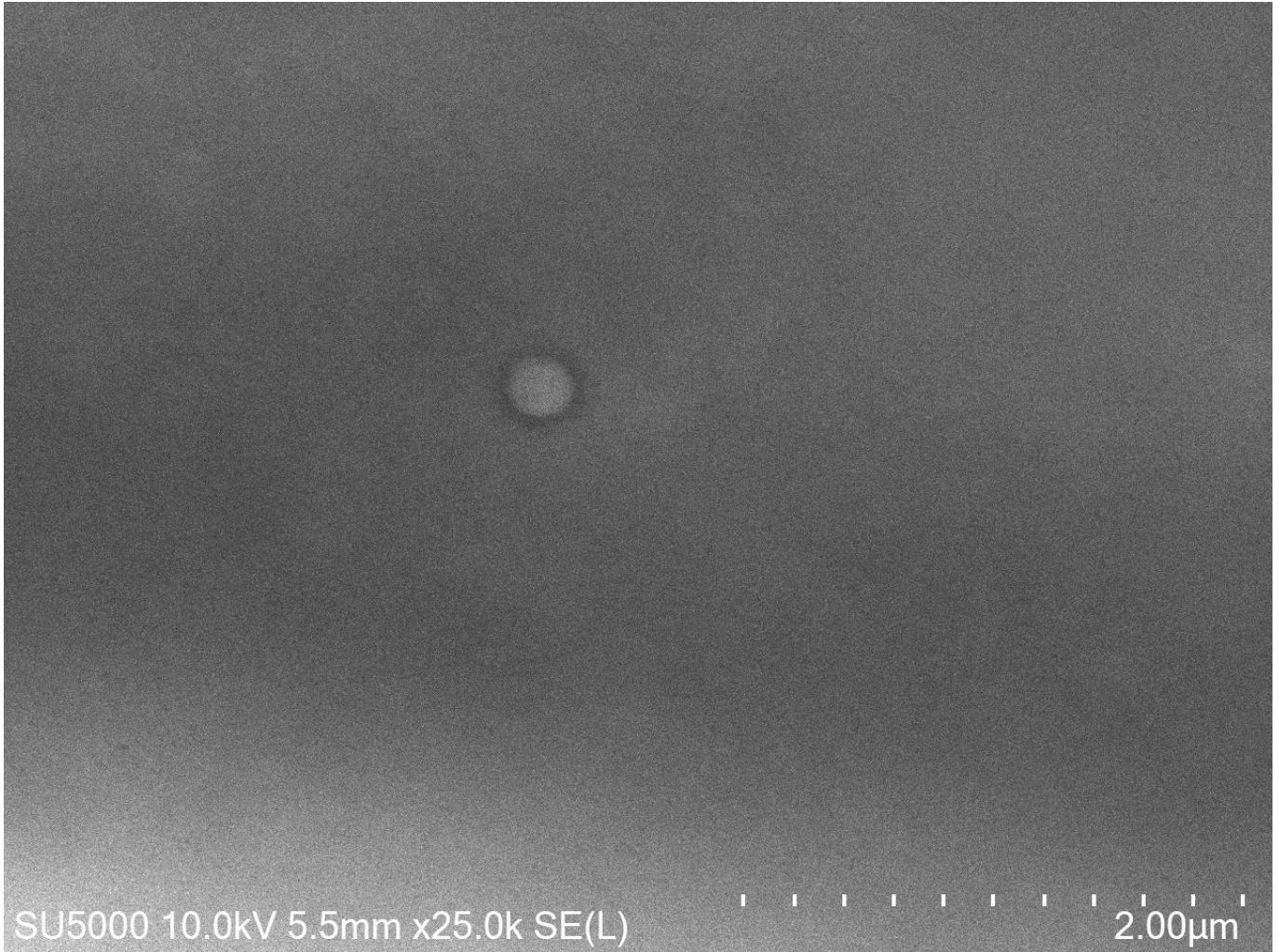




Fig. 4

